A Model for the Activation of Plasma Membrane Calcium Pump Isoform 4b by Calmodulin†

Alan R. Penheiter,‡ Željko Bajzer,‡,§ Adelaida G. Filoteo,‡ Richard Thorogate,|| Katalin Török,|| and Ariel J. Caride*,‡

Department of Biochemistry and Molecular Biology and Biomathematics Resource, Mayo Clinic, 200 First Street SW, Rochester, Minnesota 55901, and Department of Pharmacology and Clinical Pharmacology, St. George Hospital Medical School, Cranmer Terrace, London SW17 ORE, U.K.

Received November 1, 2002; Revised Manuscript Received August 11, 2003

ABSTRACT: Overexpression of the plasma membrane calcium pump (PMCA) isoform 4b by means of the baculovirus system enabled us, for the first time, to study the kinetics of calmodulin binding to this pump. This was done by stopped-flow fluorescence measurements using 2-chloro-(amino-Lys_{75})-[6-[4-(*N*,*N*-diethylamino)phenyl]-1,3,5-triazin-4-yl]calmodulin (TA-calmodulin). Upon mixing with PMCA, the fluorescence of TA-calmodulin changed along a biphasic curve: a rapid and small increase in fluorescence was followed by a slow and large decrease that lasted about 100 s. The experiment was done at several PMCA concentrations. Global fitting nonlinear regression analysis of these results led to a model in which PMCA is present in two forms: a closed conformation and an open conformation. Calmodulin reacts with both conformations but reacts faster and with higher affinity for the open conformation. Measurements of the ATPase activity of PMCA under similar conditions revealed that the open form has higher ATPase activity than the closed one. Contrasting with the reaction with the whole pump, TA-calmodulin reacted rapidly (in about 2 s) with a calmodulin-binding peptide made after the sequence of the calmodulin-binding domain of PMCA (C28). Results of TA-calmodulin binding to C28 are explained by a simpler model, in which only an open conformation exists.

Plasma membrane calcium pumps (PMCAs)[1] actively extrude Ca^{2+} across the plasma membrane. There are four genes that encode isoforms of this pump, and the variety of PMCAs is greatly enhanced by the presence of two alternative splicing sites (*1*). Isoform 4b is the most widespread, and since it is present in erythrocytes, a traditional model for the study of Ca^{2+} transport (*2*), it is the most studied isoform of the pump (*3*). All experiments in this study were performed with human isoform 4b of PMCA.

From early studies it was known that, depending on the isolation procedure, PMCA can display two types of kinetic behavior: (a) a low V_{max} and low affinity for Ca^{2+} type or (b) a high V_{max} and high affinity for Ca^{2+} type (*4*, *5*). Later, it was discovered that these differences were due to the association of PMCA with calmodulin (CaM), the main regulator of this pump (*6*, *7*). CaM increases both the affinity for Ca^{2+} and the V_{max} of PMCA (*8*). A characteristic of the activation of PMCA by CaM is that it is slow (*9*). Recently, we found that different PMCA isoforms are activated by CaM at different rates (*10*). When Ca^{2+} concentration is raised in the presence of CaM, isoforms with higher CaM activation rates react faster to Ca^{2+} as well (*11*). We have shown that this is an interesting adaptation of the different PMCAs to the speed of the Ca^{2+} signal (*11*). Moreover, dissociation of CaM from PMCA is also slow. Slow association and dissociation of CaM are responsible for the phenomenon termed "memory effect". When PMCA is subjected to two consecutive Ca^{2+} spikes, it reacts faster to the second spike than to the first one (*12*). Recently, it was pointed out that these special kinetic properties of CaM binding to PMCA are important to shape Ca^{2+} signaling in Jurkat cells (*13*).

Proteolysis (*14*), inhibition by CaM-binding peptides (*15*), and molecular biology studies (*16*) have shown that the inhibited form is caused by binding of the C-terminal tail, which includes the CaM-binding domain, to the cytoplasmic catalytic core of the enzyme (*17*, *18*). Binding of CaM relieves this inhibition. In this publication we refer to the autoinhibited form as closed and any conformation in which the autoinhibitory interaction is absent as open. The purpose of this investigation is to clarify two aspects of the mechanism of activation by CaM: First, does CaM bind exclusively to the open form, stabilizing it, or does it bind to the closed form, promoting opening? Second, is the slow activation a product of slow binding of CaM or a slow opening of the pump? To provide answers to these questions, we performed stopped-flow measurements of binding of a fluorescent derivative of CaM to PMCA and parallel measurements of ATPase activity. We present a model based on the results of these experiments.

† With support from American Heart Association Grant 30531Z to A.J.C. and from the Wellcome Trust (U.K.) to K.T. The laboratory of Dr. John T. Penniston, in which this research was conducted, is supported by NIH Grant GM 28835.

* To whom correspondence should be addressed. Tel: 507-284-4236. Fax: 507-284-9759. E-mail: caride@mayo.edu.

‡ Department of Biochemistry and Molecular Biology, Mayo Clinic.

§ Biomathematics Resource, Mayo Clinic.

|| St. George Hospital Medical School.

[1] Abbreviations: PMCA, plasma membrane calcium pump; CaM, calmodulin; TA-CaM, 2-chloro-(amino-Lys_{75})-[6-[4-(*N*,*N*-diethylamino)phenyl]-1,3,5-triazin-4-yl]calmodulin.

10.1021/bi027098+ CCC: $25.00
Published on Web 09/25/2003

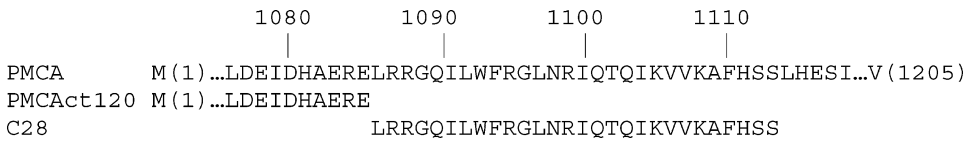

FIGURE 1: A scheme of the primary structure of PMCA4b, the truncated mutant PMCAct120, and the C28 peptide.

In many CaM-activated enzymes, including PMCA, the sequence that binds CaM can be isolated, retaining the CaM-binding properties (for a review of CaM-binding sequences, see ref *19*). Structural (*20*) and kinetic (*21*, *22*) studies with these CaM-binding sequences of different CaM-activated enzymes provided a wealth of information about the mechanism of regulation of enzymatic activity by CaM. In the case of PMCA, studies with the isolated 28-residue CaM-binding domain (C28, Figure 1) confirmed the hypothesis that this sequence acted both as an autoinhibitor and as a CaM-binding region (*15*). Here we report results of binding of TA-CaM to the C28 peptide and compare these results with those obtained with PMCA.

EXPERIMENTAL PROCEDURES

Construction of Plasmids. Plasmids pVL-1392 and pSG5-h4b were gifts from Ernesto Carafoli (University of Padova, Italy). Using *Bam*HI and *Kpn*I sites, h4b was excised from pSG5 and inserted into expression vector pVL-1392. Standard transformation and DNA purification techniques were followed.

Preparation and Amplification of Recombinant Baculovirus. Recombinant baculovirus was prepared using the Pharmingen BaculoGold transfection kit. More than 95% of the plaques were PMCA-positive with this system. Briefly, *Spodoptera frugiperda* (Sf9) cells, in Grace culture medium without fetal bovine serum, were cotransfected with 2 μg of transfer plasmid DNA and 5.0 μg of BaculoGold DNA following the manufacturer's protocol. Plaques expressing the recombinant protein were isolated by plaque assay and screened for PMCA by Western blot. The selected early viral stock was amplified using a multiplicity of infection of 0.1−0.2 following standard procedures and the titer of the amplified stock determined (*23*). The viral stock was kept at 4 °C in the dark.

Expression of PMCA and PMCAct120 in Sf9 Cells. The expression for protein production was carried out by infecting Sf9 cells in suspension in complete Grace medium with the recombinant virus at a multiplicity of infection of 1. After 48 h of incubation at 27 °C, the cells were harvested. A 500 mL culture yielded 800 $\times$ 10^6 cells. The cells were washed with PBS buffer containing 1 mM EDTA and protease inhibitors, quick frozen, and kept at −80 °C until microsome processing.

Microsomal Preparation. Crude microsomal membranes from Sf9 cells, untransfected or transfected with PMCA or PMCAct120, were prepared essentially as described previously for COS cells with some minor modifications (*24*). After the cells were washed with PBS containing increased amounts of protease inhibitors (10 μg/mL aprotinin and 4 μg/mL leupeptin), the cell pellets were immediately frozen in aliquots of 200 $\times$ 10^6 cells until processing. The volumes of buffers used for homogenizing the relatively large cell pellet were also increased 2−3 times to maintain the concentrations required to promote formation of inside-out vesicles. Per 200 $\times$ 10^6 cells, 6 mL of hypotonic and 6 mL of homogenization buffers were used. Aliquots of the microsomes were stored at −80 °C.

CaM Overlay. Sf9 microsomes (0.2 μg) expressing human PMCA were subjected to SDS−PAGE in 7.5% gels and blotted to PVDF membranes as described before (*25*). Then the blots were incubated with biotinylated CaM in the presence of PBS buffer containing 100 μM $CaCl_2$. After a 30 min incubation at room temperature, the blots were washed twice with the same solution without biotinylated CaM and developed by the peroxidase method with the ABC kit (Vector Laboratories, CA). Controls were performed in the presence of 100 μM EGTA (no Ca^{2+}).

Determination of PMCA Concentration by Gel Electrophoresis and Quantitative Staining. Total protein determination of crude membrane preparations was determined by the method of Lowry (*26*). The specific amount of PMCA in each crude membrane preparation was determined by quantitative SDS−PAGE with included BSA standards, similar to the method used for PMCA by Etcharte et al. (*27*). Twenty micrograms of total protein (5−15 μL of membrane preparation) from Sf9 cells expressing PMCA or untransfected Sf9 cells was loaded on a 7.5% polyacrylamide gel. On the same gel, a series of protein standard lanes was run with 0.25−5 μg of BSA. The gel was stained with amido black and scanned on a flat bed scanner. PMCA and BSA bands were quantified with Scion Image using equal area rectangles. Since minor amounts of endogenous Sf9 proteins were also present in the same region of the gel as the PMCA band, the density of a rectangle in the adjacent untransfected cell lane was subtracted from the PMCA band. Typical expressions yielded 0.6−2 μg of PMCA by SDS−PAGE per 20 μg of total protein by the Lowry procedure.

Western Blots. Transfer to PVDF membranes and blot staining with antibody 5F10 were performed as described in ref 25. Antibody 5F10 recognizes all isoforms of the pump (*28*).

Measurements of ATPase Activity. The ATPase activity was measured at 37 °C by continuously monitoring the absorbance at 360 nm, following the procedure outlined previously (*10*). The media contained 120 mM KCl, 30 mM TES−triethanolamine (pH 7.2), 5 mM $MgCl_2$, 200 μM EGTA, 2.5 mM ATP, 0.2 mM 2-amino-6-mercapto-7-methylpurine, 1 unit/mL purine nucleoside phosphorylase, 5 mM NaN_3, 1 mM dithiothreitol, 0.5 mM ouabain, 4 μg/mL oligomycin, 200 nM thapsigargin, 2 μg/mL aprotinin, 0.5 μg/mL leupeptin, CaM (in the concentration indicated in the legend of the figures), and enough $CaCl_2$ to obtain the concentration of free Ca^{2+} indicated in the legend of the figures. Free Ca^{2+} was calculated as described in refs *29* and *30*. Results of these calculations are nearly identical to those obtained with Maxchelator (www.stanford.edu/Íjcpatton/maxc.html).

Origin and Preparation of Reagents. TA-cal was synthesized by labeling human liver calmodulin expressed in

Escherichia coli and purified by HPLC in K. Török's laboratory as previously described for pig brain calmodulin (*22*). The labeled site was previously identified as Lys75 by gas-phase microsequencing of labeled tryptic fragments Lys75-Met76-Lys77 and Lys75-Arg86 (K. Török, S. Howell, A. Aitken, and D. R. Trentham, unpublished data). HPLC-purified TA-cal appeared as a single peak by UV detection at 215 nm and fluorescence detection with excitation at 365 nm and emission at 420 nm (data not shown). TA-CaM was analyzed by mass spectrometry using a Kratos MALDI-TOF mass spectrometer at SGHMS Proteomics Facility, London. MALDI-TOF of HPLC-purified TA-cal identified an average mass of 16966.7 Da, consistent with the incorporation of a single TA moiety (261.7 Da) in each calmodulin molecule (16706.4 Da) to give a theoretical mass of 16968.1 Da. In this preparation the labeled fragments Lys75-Met76-Lys77 and Lys75-Arg86 were recovered from complete tryptic digestion as in previous work in which Lys75 was identified as the labeled residue.

Peptide C28 was synthesized in the Mayo Protein Core Facility and purified to homogeneity by HPLC. The sequence of the peptide is given in Figure 1.

Binding of TA-CaM to PMCA. Stopped-flow measurements of changes in fluorescence of TA-CaM were performed in an Applied Photophysics SX.18MV reaction analyzer. The excitation wavelength was 365 nm, and the emitted light was detected using a 390 nm cutoff filter. The syringes contained the concentrations of TA-CaM and PMCA or C28 peptide indicated in the legend of the figures in media containing 30 mM Tes−TEA (pH 7.2), 120 mM KCl, 5 mM $MgCl_2$, 0.2 mM EGTA, and enough $CaCl_2$ to obtain 10 μM free Ca^{2+}. Measurements were performed at 37 °C so they were directly comparable to the ATPase activity results.

Data Analysis. Individual curves were fitted by nonlinear regression using the GraphPad Prizm software. When global analysis was performed, different models were fitted by using the Dynafit software (Biokin, Inc.) (*31*) (with local offset option to compensate for possible instrument voltage drift), and corroborated by analysis using the M-LAB platform (*32*).

RESULTS

Since the experiments were carried out in a crude microsomal preparation from Sf9 cells in which PMCA was overexpressed, it was necessary to verify that PMCA is the only CaM-binding protein present in these microsomes. For this purpose, this preparation was run on an SDS−PAGE gel, transferred to PVDF membranes, and incubated either with antibody 5F10 (to identify PMCA) or with biotinylated CaM in the presence of 100 μM Ca^{2+} or without Ca^{2+}. The blots were then developed to detect bound CaM. Figure 2A (lane 1) shows that the microsomal preparation has a main band at about 135 kDa. Quantitation of this band indicated that it contains about 10% of the protein loaded. Lane 2 shows that a Western blot with antibody 5F10 confirmed the identity of this band as a PMCA. There are also minor proteolytic fragments of PMCA as reported previously (*28*). Lane 3 shows that the only band that bound CaM had the expected size for PMCA. Lane 4 shows that no binding was detected in the absence of Ca^{2+}. Figure 2B shows a typical trace of an experiment in which a microsomal preparation containing 50 nM PMCA was mixed with 17 nM TA-CaM.

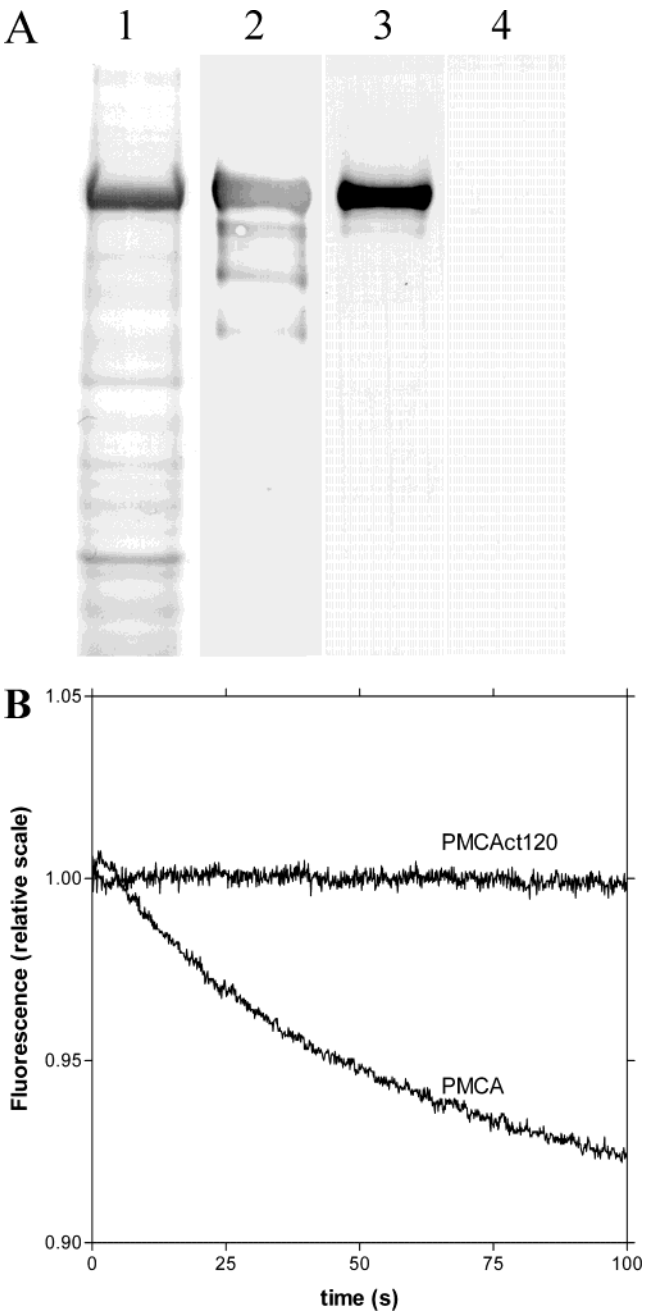

FIGURE 2: (A) Lane 1: Coomassie Blue staining of 10 μg of Sf9 cell membranes in which PMCA4b was overexpressed. Lane 2: Western blot of 200 ng of the same membranes. Lane 3: Biotinylated calmodulin overlay of the same Sf9 cell membranes in the presence of 100 μM Ca^{2+}. The membrane protein (200 ng) was loaded onto a 7.5% gel, subjected to electrophoresis, and transferred to PVDF membranes. Conditions for incubation with biotinylated calmodulin (in the absence and in the presence of Ca^{2+}) and staining are described in Experimental Procedures. Lane 4: Same membranes subjected to calmodulin overlay but in the presence of 100 μM EGTA. (B) Time course of fluorescence changes when 17 nM TA-CaM was mixed with microsomes containing either 50 nM PMCA or 50 nM PMCAct120. The photomultiplier voltage was set at 523 V in both cases.

There is a fast, small increase in fluorescence followed by a slow, decreasing phase. In the same figure, we show the results of mixing 17 nM TA-CaM with a microsomal preparation containing 50 nM PMCAct120. This is a truncated mutant of PMCA that is fully active but lacks the 120 C-terminal residues and thus lacks the calmodulin-

binding region (see Figure 1). As shown in Figure 2B, there was no change in fluorescence in this case. Control experiments also showed no detectable fluorescence changes either when TA-CaM was mixed with PMCA in the absence of Ca^{2+} or when TA-CaM was mixed with buffer but no PMCA. Therefore, we concluded that, in our experiments, the changes in fluorescence of TA-CaM were only due to binding to the calmodulin-binding region of PMCA. On the basis of these results, we performed the experiments using the crude microsomal preparation without further purification. This is important because it enabled us to observe PMCA inserted in eukaryotic cell membranes, without the addition of detergents or exogenous phospholipids, which might otherwise alter the properties of this pump (*33*). Purified PMCA could not be used in these experiments because when PMCA is removed from the membrane, it dimerizes at the high concentrations required for the stopped-flow experiments. Dimerization involves the C-terminal CaM-binding tail and abolishes autoinhibition and thus abolishes CaM activation (*34*, *35*). It is worth pointing out that in a previous publication we demonstrated that PMCA 4b expressed in Sf9 cells shows the same characteristics regarding Ca^{2+} affinity and activation by calmodulin as the erythrocyte enzyme or the enzyme expressed in COS cells (*12*).

Figure 3 summarizes the characteristics of the activation of PMCA by TA-CaM, as compared to unmodified CaM. TA-CaM activated PMCA to an extent similar to that of unmodified CaM. The maximal activity of PMCA in these experiments was approximately 0.5 μmol min^{-1} (mg of membrane protein)$^{-1}$. This value is almost 2 orders of magnitude higher than the values obtained in preparations from COS cells [5−8 nmol min^{-1} mg^{-1} (*16*)] or erythrocyte membranes (20 nmol min^{-1} mg^{-1}) (*36*). When the activity of Sf9 cell preparations is expressed per milligram of PMCA protein, the value is 5 μmol min^{-1} mg^{-1}, which is similar to the value reported by Niggli et al. for the enzyme purified from human erythrocytes (*36*). The apparent affinity was slightly higher for TA-CaM (K_d for the activation was 4.8 ± 1.1 nM for TA-CaM and 11.6 ± 2.4 nM for CaM) (Figure 3A). We also measured k_{act}, the apparent rate constant for PMCA activation, as a function of either TA-CaM or CaM concentration. A plot of k_{act} as a function of either TA-CaM or CaM concentration can be fitted with the same straight line. The slope was $(3.1 \pm 0.1) \times 10^{-4}$ M^{-1} s^{-1}. Thus, TA-CaM and CaM activate PMCA in very similar fashion. As a whole, these results reinforce the validity of using TA-CaM as a probe to study the binding of CaM to PMCA and confirm the suitability of our PMCA preparation.

In the experiment in Figure 4A, we analyzed the time course of TA-CaM binding to PMCA (assessed by the change in fluorescence emission by TA-CaM) at different concentrations of PMCA. At all PMCA concentrations, the biphasic curve was characterized by a rapid small increase in fluorescence followed by a slow, large decrease. Both the early and the late phases were PMCA concentration dependent. When the experiment was repeated in the presence of 100 μM Ca^{2+} and no EGTA, results were identical. The magnitude of the early phase decreased with increasing PMCA, and the late phase appears to be faster at higher PMCA concentrations. By using global fitting to all the progression curves at different PMCA concentrations, we were able to try several models of reaction. The one that

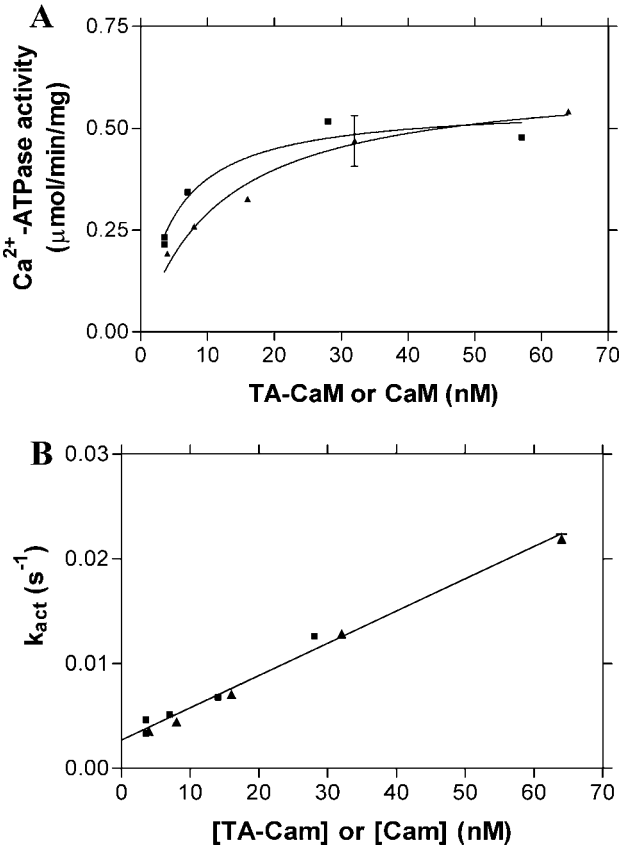

FIGURE 3: v_c (panel A) and k_{act} (panel B) as a function of calmodulin or TA-calmodulin. v_c is the increase in activity of PMCA generated by CaM or TA-CaM, and k_{act} is the observed rate constant for activation of the ATPase by CaM or TA-CaM. The values of v_c and k_{act} were taken from experiments in which the time course of the increase in activity by addition of CaM or TA-CaM was measured (for an example, see Figure 6B). Equation 1 (see Results section) was fitted to the data. The activity in the absence of CaM was 0.10 ± 0.01 μmol (mg of protein)$^{-1}$ min^{-1}. ATPase activity was measured as described in Experimental Procedures. The PMCA4b concentration was 15 nM, and the Ca^{2+} concentration was 10 μM. Key: (■) TA-CaM; (▲) CaM.

gave the best fit is shown in Figure 4C. In this model, $PMCA_c$ is the closed conformation of the pump, $PMCA_o$ is the open conformation, and $PMCA_{o*}$ is open conformation after CaM isomerization. The rate constant values that were obtained when this model was fitted to the results in Figure 4A are summarized in Table 1. Including reversibility in the last step actually made the fitting poorer and more unstable. For this reason, the last step was assumed to be irreversible.

The model presented above predicts a slow dissociation of CaM from PMCA that proceeds in several steps. To verify this prediction, we measured the dissociation of TA-CaM from PMCA. Results are presented in Figure 4B. TA-CaM fluorescence increased with a half-time of approximately 10 min. The reaction was best fitted by the sum of two exponential equations, one with an amplitude of about 10% of the total fluorescence increase and a $k_{obs1} = 0.0073$ s^{-1} and a slow component of about 90% of the fluorescence and a $k_{obs2} = 0.0015$ s^{-1}. The low value of this constant is close to the value of k_{-3} for the model proposed in the preceding paragraph. As a whole, the result in Figure 4C confirms the prediction of the model presented in Figure 4B.

In Figure 5 we compared the results of the experiment in Figure 4A with the best fit obtained with different models:

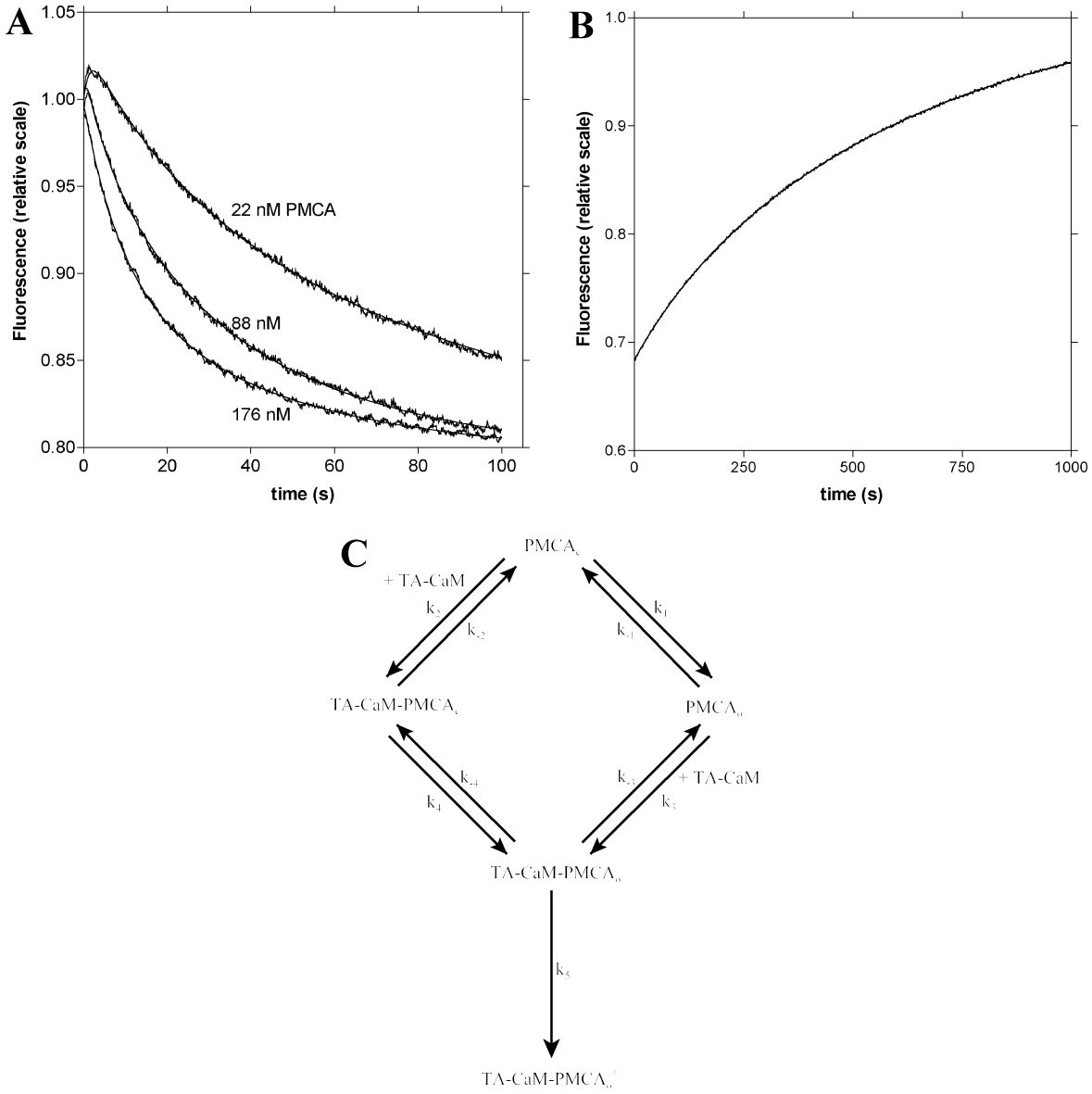

FIGURE 4: (A) Time course of binding of TA-calmodulin to PMCA4b. The pump was expressed in Sf9 cells. The TA-calmodulin concentration was 17 nM, and the PMCA concentration was 22, 88, and 176 nM. All other concentrations were as described in Experimental Procedures. The photomultiplier voltage in this experiment was set at 445 V. The fitting of the model shown in panel B to the data was obtained by using Dynafit software (*26*). The fitting lines represent $F(t) = r_{\text{TA-CaM}}[\text{TA-CaM}] + r_{\text{TA-CaM-PMCA}_c}[\text{TA-CaM-PMCA}_c] + r_{\text{TA-CaM-PMCA}_o}[\text{TA-CaM-PMCA}_o] + r_{\text{TA-CaM-PMCA}_{o^*}}[\text{TA-CaM-PMCA}_{o^*}]$, where relative quantum yields were denoted by the letter *r*. (B) Time course of TA-calmodulin dissociation from PMCA. TA-calmodulin (17 nM) was premixed with 50 nM PMCA. At time = 0, 1 μM calmodulin (final concentration) was mixed, and the fluorescence was recorded. The photomultiplier voltage was 523 V. (C) Scheme showing the model used to fit the data presented in panel A.

a model in which TA-CaM binds only to the closed conformation, destabilizing it (Figure 5A,C), and another in which TA-CaM binds to the open conformation, stabilizing it (Figure 5B,D). The first obvious observation is that the best fit to either of these two models fails to account for the early increase in fluorescence. Since theoretically either of these two models should be able to account for a biphasic fluorescence trace, we force the parameters to account for such a pattern. We show in Figure 5E a fit of PMCA forced to a linear model such as the one used for C28. The k, k_{-1}, and relative fluorescence of the high fluorescence intermediate were obtained from a fit to the 22 nM data set alone, these constants were then fixed, and a global fit was performed. In that case, we can get a reasonably good fit for the time curve at 22 nM, but in the curves at higher pump concentration the features of the curve are grossly exaggerated, and the early fluorescence peak increases instead of decreasing with increasing PMCA concentrations. Therefore, we discarded the linear models and chose the branched model presented in Figure 4.

In the experiment corresponding to Figure 6, we compared the rate of TA-CaM binding to PMCA with the rate of activation of PMCA by TA-CaM. Upon mixing of 17 nM TA-CaM with 17 nM PMCA, TA-CaM fluorescence increased slightly and then slowly decreased (Figure 5A). The apparent rate constants for these processes were $k_{\text{obs1}} = 1.32 \pm 0.12\ \text{s}^{-1}$ and $k_{\text{obs2}} = 0.018 \pm 0.002\ \text{s}^{-1}$, respectively. In Figure 5B, the activation of 15 nM PMCA by 17 nM TA-CaM is shown. TA-CaM activated the enzyme slowly. The activation curve was fitted by an equation that was used to

Table 1: Kinetic Parameters of the Models Used for Fitting the Binding Data Shown in Figures 4−6

	PMCA			C28	
parameter	branched model	open only	closed only	three step	two step
sum of square errors	2.57×10^{-6}	3.57×10^{-5}	6.06×10^{-5}	2.4×10^{-4}	7.76×10^{-4}
k_1	0.0016 ± 0.0004 s^{-1}	0.0267 ± 0.0024 s^{-1}	0.61 ± 3.2 s^{-1}	$(4.6 \pm 0.8) \times 10^8$ s^{-1} M^{-1}	$(6.28 \pm 0.78) \times 10^9$ s^{-1} M^{-1}
k_{-1}	0.024 ± 0.014 s^{-1}	0.91 ± 1.6 s^{-1}	1 ± 4.6 s^{-1}	1100 ± 130 s^{-1}	1100 ± 5100 s^{-1}
k_2	$(3.0 \pm 0.3) \times 10^7$ s^{-1} M^{-1}		$(1.4 \pm 5.1) \times 10^8$ s^{-1} M^{-1}	600 ± 110 s^{-1}	100 ± 79 s^{-1}
k_{-2}	0.187 ± 0.006 s^{-1}		5.2 ± 27 s^{-1}	53 ± 0.6 s^{-1}	40 ± 10 s^{-1}
k_3	$(1.47 \pm 0.14) \times 10^8$ s^{-1} M^{-1}	$(1.6 \pm 2.2) \times 10^9$ s^{-1} M^{-1}		15 ± 0.6 s^{-1}	
k_{-3}	0.0005 ± 0.007 s^{-1}	0.68 ± 0.93 s^{-1}		8.7 ± 0.2 s^{-1}	
k_4	0.034 ± 0.005 s^{-1}		0.17 ± 0.49 s^{-1}		
k_{-4}	0.010 ± 0.0008 s^{-1}		0.24 ± 0.34 s^{-1}		
k_5	0.024 ± 0.003 s^{-1}	0.0481 ± 0.0006 s^{-1}	0.21 ± 0.65 s^{-1}		
r_{TA-CaM}	0.0588	0.0588	0.0588	0.0588	0.0588
$r_{TA-CaM-4b_c}$	0.0781 ± 0.0011		0.063 ± 0.003		
$r_{TA-CaM-4b_o}$	0.008 ± 0.006	0.052 ± 0.001	0.028 ± 0.099		
$r_{TA-CaM-4b_{o*}}$	0.00188 ± 0.0004	0.0059 ± 0.0001	0.0056 ± 0.0012		
$r_{TA-CaM-C28}$				0.252 ± 0.031	0.133 ± 0.001
$r_{TA-CaM-C28*}$				0.0047 ± 0.0017	0.00005 ± 0.0008
$r_{TA-CaM-C28\#}$				<0.0001	

describe the time course of ATP hydrolysis by PMCA upon addition of CaM (*10*). This equation is

$$P(t) = P_0 - v_c/k_{act} + (v_0 + v_c)t + (v_c/k_{act}) \exp(-k_{act}t) \quad (1)$$

where P_0 is the amount of product at $t = 0$, v_0 is the activity in the absence of calmodulin, v_c is the increase in activity due to the addition of TA-CaM, and k_{act} is the time constant for the change in activity.

k_{act} in this experiment was 0.025 ± 0.0004 s^{-1}. The value for k_{act} is close to the value of k_2, suggesting that the activation of the pump and the decrease in fluorescence of TA-CaM occur during the same time frame. To further test the validity of the model of activation by CaM, we simulated the time course of change in ATPase activity by using the constants obtained in the experiment in Figure 4, and we compared it with the experimental change in the ATPase activity of PMCA upon mixing with 17 nM TA-CaM. Results are shown in Figure 4C. The increase in ATPase activity was best fitted by the model simulation when we considered that all of the open forms have high ATPase activity and that the closed forms have 10% of the activity of the open forms. These estimations were based on data of CaM activation of PMCA (*10*, *16*). When we considered that TA-CaM-4b$_{o*}$ was the only species with high ATPase activity, the simulation showed an activation that was too slow to fit the experimental data. The species 4b$_o$ was present initially but decreased rapidly; therefore considering whether 4b$_o$ has high or low ATPase activity made little difference in the simulations. The results suggest that the three open forms (4b$_o$, TA-CaM-4b$_o$, and TA-CaM-4b$_{o*}$) have high ATPase activity. Therefore, the last step in the model presented in Figure 4B is necessary to fit the fluorescence results but does not result in additional activation of PMCA.

CaM-binding peptides have been widely used in kinetic studies for modeling the interaction of CaM with its many different targets, including PMCA (*15*, *22*, *37*−*39*). In an effort to better understand the binding of CaM to PMCA, we analyzed the binding of TA-CaM to the peptide C28. The results of this experiment are shown in Figure 7A. The first observation is that the reaction of TA-CaM with C28 is much faster that the reaction with the full-length PMCA. Even at the lowest peptide concentration, the reaction was completed in about 2 s (compare it to the 100 s scale used in Figures 4 and 6). As in the reaction of TA-CaM with PMCA, there was an initial increase in fluorescence followed by a decaying phase. Again, the initial phase was extremely fast, lasting only a few milliseconds. However, the increase in fluorescence is magnified at higher C28 concentrations, which is opposite to what we found when TA-CaM bound to the whole PMCA. The time course of the decaying phase of the reaction could not be fitted to a simple exponential decay, indicating the presence of additional steps. Of several models we tried, we found that the model included in Figure 7B provided the best fit. The constants that gave the best fit, as well as the SSE, are given in Table 1 (three-step model). In Figure 7C we show the fit of the same experimental data to a simplified, two-step model, which is shown in Figure 7D. As mentioned before, it is clear that in this case the fit of the two-step model to the experimental data is poor, especially in the decreasing phase. This is reflected in a 5-fold increase in the SSE. Therefore, we chose the three-step model to interpret the data.

DISCUSSION

The combination of measurements of kinetics of CaM binding, ATPase activity, and the use of global nonlinear regression analysis allowed us to propose a model for CaM activation of PMCA. The model assumes that the pump is present in two states: open and closed. The open forms have high ATPase activity and high affinity for Ca^{2+}, while the closed forms have low activity and low affinity for Ca^{2+}. The ratio of the rate constants k_1/k_{-1} (see Figure 4B and Table 1) implies that in the absence of CaM most of the enzyme is in the closed form. According to the model, CaM can bind to both open and closed forms but binds faster to the open form and dissociates at a slower rate from it. After binding, the open form undergoes two isomerization steps. These isomerization steps were a necessary addition to obtain a

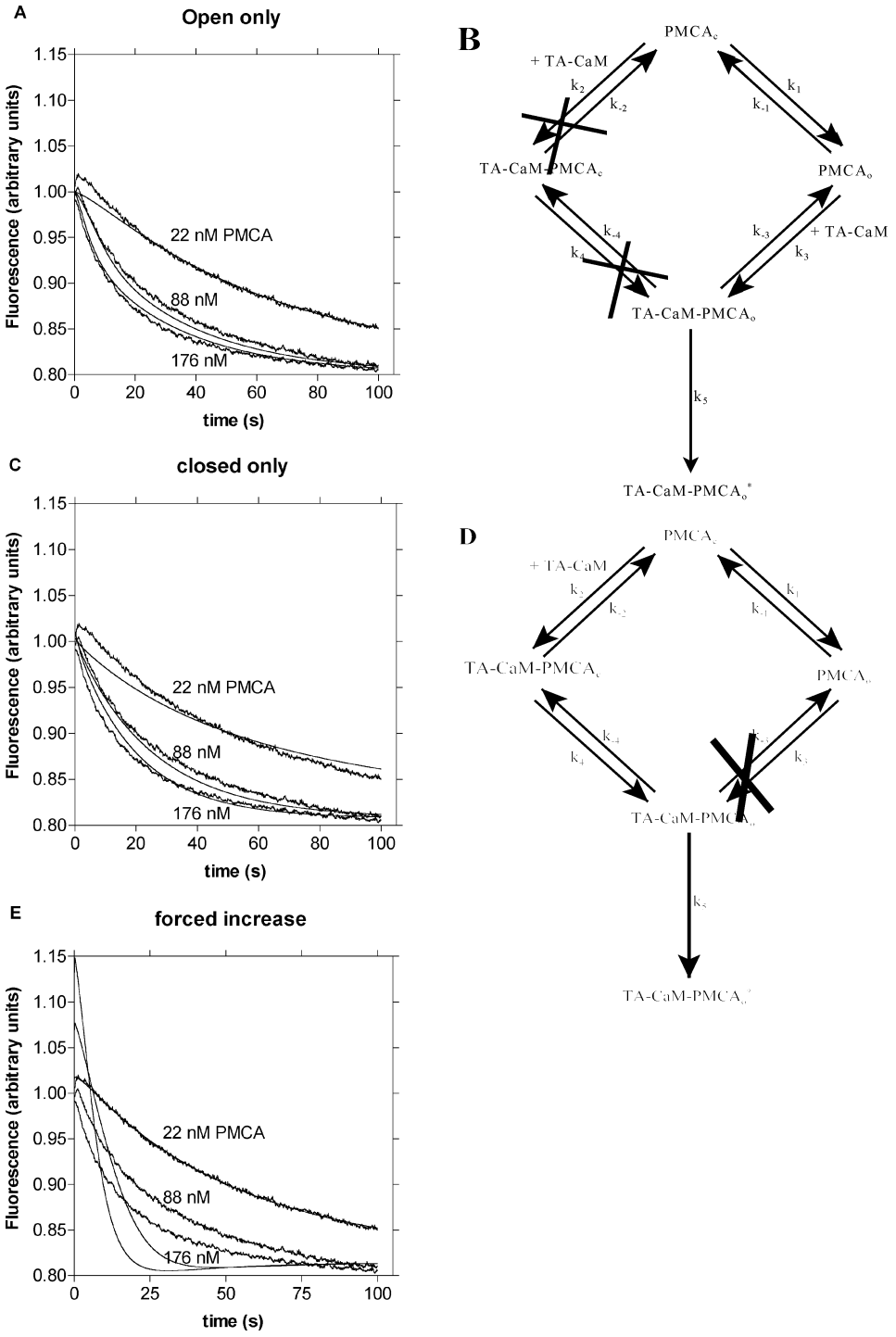

FIGURE 5: Fitting of alternative models to the data presented in Figure 4A. (A) Fitting to the model presented in panel B. (B) Model in which TA-CaM binds only to the open form of PMCA. (C) Fitting to the model presented in panel D. (D) Model in which TA-CaM binds only to the closed form of PMCA. (E) Fitting to the open only model, in which the parameters were obtained from fitting the 22 nM PMCA curve and then used to fit the rest of the curves. The same results were obtained when this procedure was used for the closed only model.

plausible fit to the fluorescence data. This is also expected, since CaM is known to bind to its targets in a sequential manner, the C-terminal lobe binding first and the N-terminal lobe binding afterward (*40*).

Other models were tried, but none of them fitted the data as well as this one. For example, among the models considered, we explored the binding of TA-CaM exclusively to the open form, thus displacing the equilibrium toward this form. This model failed to reproduce the initial rise in fluorescence while giving a reasonable fit to the decreasing phase. A model in which CaM binds exclusively to the closed form, destabilizing it, was also considered. This model also gave a poor fit. Oligomerization of PMCA was reported in purified and solubilized preparations (*41*, *42*), although its demonstration in native membranes remains elusive. Accounting for dimerization does not improve fitting. In fact, it makes the fit poorer, suggesting that if dimerization of PMCA occurs in membranes, it does not impede CaM binding. This is in agreement with the available experimental evidence (*41*, *43*). We also tried models in which TA-CaM would bind to a small fraction of denatured enzyme, which would account for the early increase in fluorescence.

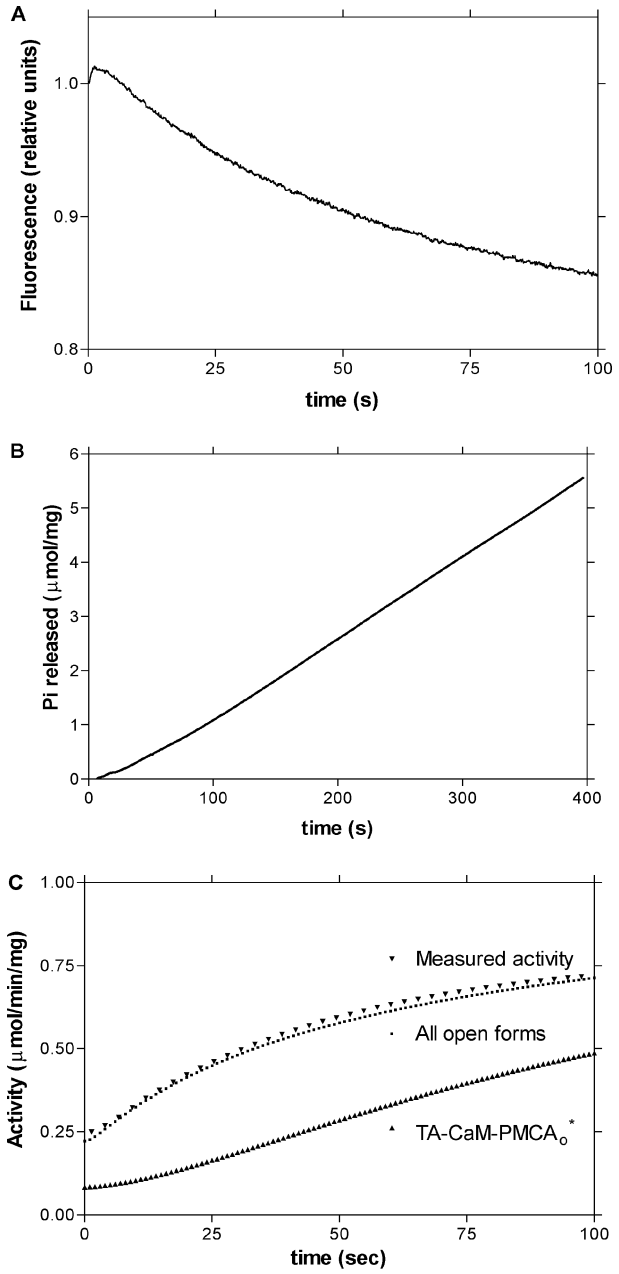

FIGURE 6: Correlation between changes in fluorescence of TA-calmodulin and activation of PMCA. Panel A: Binding of 17 nM TA-calmodulin to 17 nM PMCA4b. The free Ca^{2+} concentration was 10 μM. Panel B: Time course of ATP hydrolysis under conditions similar to those in panel A, except that the concentration of PMCA was 15 nM. The experiment was started by the addition of 17 nM TA-calmodulin. Other conditions were as described in Experimental Procedures. The free Ca^{2+} concentration was 10 μM. Panel C: Derivative of ATP hydrolysis shown in panel B compared with a simulation of the increase in ATPase activity according to the model proposed in the text. The lines were calculated by using the rate constants fitted to the data in Figure 4. Dots: Derivative of the ATPase activity shown in panel B. The activity of the closed forms was assumed to be 10% of the activity of the open forms. It was assumed that there is a background activity (in the absence of Ca^{2+}) that is 10% of the total activity, in concordance with the experimental data.

However, simulations of this model resulted in activity levels that were lower than those experimentally observed. In summary, global fitting capabilities allowed for the trial and rejection of several complex models on the basis of fitting to the experimental results.

Our interpretation of the results is consistent with observations made in other CaM-dependent enzymes: in the case of TA-CaM binding to CaM-kinase II there is also an early increase in fluorescence (of about 12%) that was interpreted as binding of one lobe of CaM without change in CaM structure. Such interpretation is consistent with our findings (*39*).

From the values of the constants fitted for the model described for PMCA, it appears that the limiting step for the activation is the opening of the pump, determined by k_1 and k_4 (Figure 4B). Except for a very brief overshoot, during which $4b_o$ exists in significant concentration, the activation upon TA-CaM binding is characterized by the appearance of TA-CaM-$4b_o$ and TA-CaM-$4b_{o*}$. The proposed mechanism is branched: a fraction of the enzyme would exist in the open form even in the absence of CaM and would be stabilized by CaM. On the other hand, the fraction of the enzyme that is in the closed form would bind CaM first, and the complex CaM-$4b_c$ would open. On the basis of the estimated rate constants obtained from the experiments in Figures 4 and 5, the preferred route would be the second one. In both routes, the limiting step seems to be the opening of the enzyme. The rationale behind a branched mechanism is that it is not possible to fit data in which the initial increase in fluorescence becomes smaller with increasing PMCA concentrations with a linear sequence of reactions, as we showed in Figure 5. In a recent paper, Gao et al. (*44*) found that CaM in which Met residues have been oxidized binds to the same sequence in PMCA but fails to activate. This is in keeping with our idea that CaM may bind to the closed form of PMCA, destabilizing it. Oxidized CaM would fail to destabilize it.

The ratio k_{-1}/k_1 gives the ratio of concentrations between closed and open forms in the absence of CaM, and it is about 15. Therefore, if the closed form had no ATPase activity, then CaM would activate PMCA 15-fold. Typically, PMCA is activated by CaM about 5−10 times at saturating Ca^{2+} concentrations (for example, see refs *12* and *45*). The most likely explanation is that the closed form has a low level of ATPase activity. In the simulations in Figure 6C we assume that the closed form has 10% of the activity of the open forms. The alternative possibility that this low activity is due to the presence of trace amounts of proteolytically activated enzyme can be ruled out by the well-known fact that CaM increases the apparent affinity for Ca^{2+} as well as the maximal activity (*15*).

Although the design of the experiment in Figure 4 is not adequate to calculate dissociation rates, it is encouraging that the fit estimates a very low value for k_{-3}, the dissociation of CaM. When the rate of dissociation of TA-CaM was measured directly (Figure 4B), it was compatible with the slow rate of dissociation predicted by our model. Furthermore, this value is in agreement with the values we found for the inactivation of the pump upon CaM removal (*10*, *12*). TA-CaM was used in the past to study binding of CaM to MLCK (*22*, *38*). Results of the stopped-flow studies of TA-CaM binding to the MLCK CaM-binding peptide and C28 showed similarities: both revealed an early increase in fluorescence followed by a slower decrease. However, a striking difference is that TA-CaM, while it inhibited CaM-dependent MLCK, activated the plasma membrane calcium pump in a manner almost identical to that of native CaM.

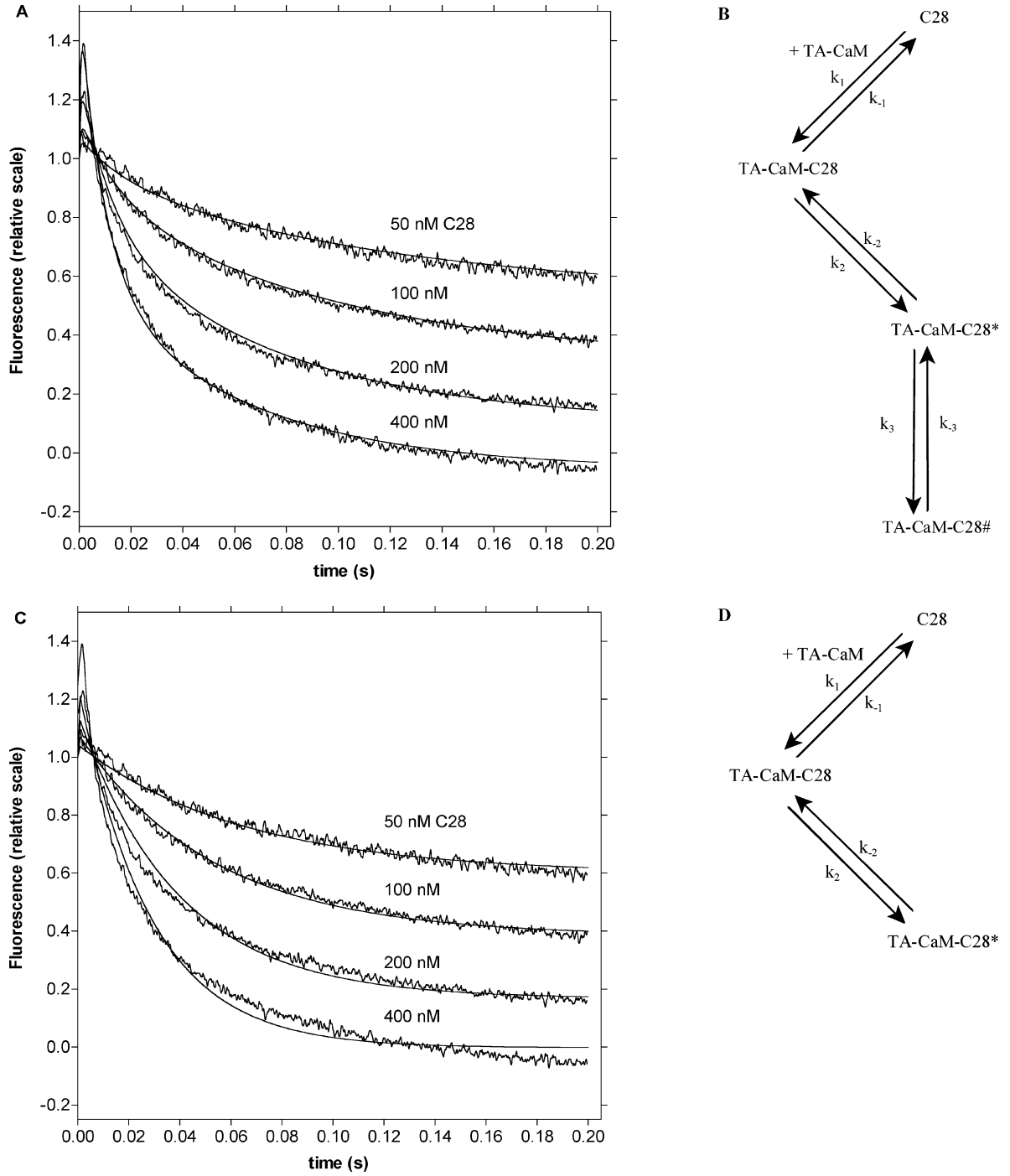

FIGURE 7: (A) Time course of binding of TA-calmodulin to the C28 peptide. The TA-calmodulin concentration was 17 nM. Peptide concentrations are indicated in the figure. The free Ca^{2+} was 10 μM. All other concentrations are as indicated in Experimental Procedures. The photomultiplier voltage was 537 V. The model proposed in panel B was fitted to the experimental data. The fitting line represents $F(t) = r_{TA-CaM}[TA\text{-}CaM] + r_{TA-CaM-C28}[TA\text{-}CaM\text{-}C28] + r_{TA-CaM-C28*}[TA\text{-}CaM\text{-}C28^*] + r_{TA-CaM-C28\#}[TA\text{-}CaM\text{-}C28\#]$, where r denotes the relative quantum yield of each of the species considered. (B) Three-step model used to fit the data in panel A. (C) The same data shown in panel A when fitted by the two-step model shown in panel D. (D) Two-step model.

Studies on the binding of TA-CaM to C28 revealed a much faster overall reaction than binding to the whole enzyme. The results could be fitted to a much simpler mechanism also. This faster binding can be explained on the basis that the peptide is free in solution and there is no physical restriction for its binding to CaM. Interestingly, the data were best fitted by a model that showed three phases during CaM binding. They are likely to represent the three different steps that were previously described during CaM binding for a number of CaM-binding peptides (*46*, *47*): binding of the C-terminal lobe of CaM, binding of the N-terminal lobe, and collapse of CaM around the CaM-binding domain.

It is tempting to compare the steps of the proposed mechanisms of TA-CaM binding to C28 and to the whole PMCA in terms of structural similarity. However, this comparison should be done with caution because of the obvious restrictions that the rest of the PMCA structure may impose and that are not present in the case of the peptide.

When individual steps are compared, the limiting step in the activation of PMCA by TA-CaM is the transition from

closed to open conformation. Binding of TA-CaM to the open conformation of PMCA was only 3 times slower than binding to the peptide (compare k_3 in the model for the reaction to the whole pump with k_1 of the reaction with C28). On the other hand, the transitions governed by k_1 and k_4 (in the model for binding of TA-CaM to PMCA) seem to be the slow steps of the process.

Taking the above-mentioned conclusion into account, it is plausible to suggest that the slower reaction of CaM with the whole PMCA (as compared to the reaction with C28) is due to the restrictions imposed by the binding of the CaM-binding domain to its binding site in the core of the pump. The restrictions can have two causes: (1) slow dissociation of the CaM-binding domain from its site in the core of the cytoplasmic domain of the pump (*45*); (2) slow activation due to the tethering of the CaM-binding domain to the pump (*48*). Further work on the CaM-binding region is necessary to clarify this point.

ACKNOWLEDGMENT

A. J. Caride thanks Dr. John T. Penniston for critical reading of the manuscript and for enthusiastic support.

REFERENCES

1. Strehler, E. E., and Zacharias, D. A. (2001) *Physiol. Rev. 81*, 21−50.
2. Schatzmann, H. J. (1983) *Annu. Rev. Physiol. 45*, 303.
3. Strehler, E. E., James, P., Fischer, R., Heim, R., Vorherr, T., Filoteo, A. G., Penniston, J. T., and Carafoli, E. (1990) *J. Biol. Chem. 265*, 2835−2842.
4. Scharff, O. (1976) *Biochim. Biophys. Acta 442*, 206.
5. Scharff, O., and Foder, B. (1978) *Biochim. Biophys. Acta 509*, 67−77.
6. Jarrett, H. W., and Penniston, J. T. (1977) *Biochem. Biophys. Res. Commun. 77*, 1210−1216.
7. Gopinath, R. M., and Vincenzi, F. F. (1977) *Biochem. Biophys. Res. Commun. 77*, 1203−1209.
8. Enyedi, Á., Flura, M., Sarkadi, B., Gardos, G., and Carafoli, E. (1987) *J. Biol. Chem. 262*, 6425−6430.
9. Scharff, O., and Foder, B. (1982) *Biochim. Biophys. Acta 691*, 133−143.
10. Caride, A. J., Elwess, N. L., Verma, A. K., Filoteo, A. G., Enyedi, Á., Bajzer, Z., and Penniston, J. T. (1999) *J. Biol. Chem. 274*, 35227−35232.
11. Caride, A. J., Filoteo, A. G., Penheiter, A. R., Pászty, K., Enyedi, Á., and Penniston, J. T. (2001) *Cell Calcium 30*, 49−57.
12. Caride, A. J., Penheiter, A. R., Filoteo, A. G., Bajzer, Z., Enyedi, Á., and Penniston, J. T. (2001) *J. Biol. Chem. 276*, 39797−39804.
13. Bautista, D. M., Hoth, M., and Lewis, R. S. (2002) *J. Physiol. 541*, 877−894.
14. Zurini, M., Krebs, J., Penniston, J. T., and Carafoli, E. (1984) *J. Biol. Chem. 259*, 618−627.
15. Enyedi, Á., Vorherr, T., James, P., McCormick, D. J., Filoteo, A. G., Carafoli, E., and Penniston, J. T. (1989) *J. Biol. Chem. 264*, 12313−12321.
16. Enyedi, Á., Verma, A. K., Heim, R., Adamo, H. P., Filoteo, A. G., Strehler, E. E., and Penniston, J. T. (1994) *J. Biol. Chem. 269*, 41−43.
17. Falchetto, R., Vorherr, T., Brunner, J., and Carafoli, E. (1991) *J. Biol. Chem. 266*, 2930−2936.
18. Falchetto, R., Vorherr, T., and Carafoli, E. (1992) *Protein Sci. 1*, 1613−1621.
19. Rhoads, A. R., and Friedberg, F. (1997) *FASEB J. 11*, 331−340.
20. Crivici, A., and Ikura, M. (1995) *Annu. Rev. Biophys. Biomol. Struct. 24*, 85−116.
21. Bayley, P. M., Findlay, W. A., and Martin, S. R. (1996) *Protein Sci. 5*, 1215−1228.
22. Török, K., and Trentham, D. R. (1994) *Biochemistry 33*, 12807−12820.
23. O'Reilly, D. R., Miller, L. K., and Luckow, V. A. (1994) *Baculovirus Expression Vector*, Oxford University Press, New York.
24. Verma, A. K., Enyedi, Á., Filoteo, A. G., Strehler, E. E., and Penniston, J. T. (1996) *J. Biol. Chem. 271*, 3714−3718.
25. Filoteo, A. G., Enyedi, Á., Verma, A. K., Elwess, N., and Penniston, J. T. (2000) *J. Biol. Chem. 275*, 4323−4328.
26. Lowry, O. H., Rosebrough, N. J., Farr, A. L., and Randall, R. J. (1951) *J. Biol. Chem. 193*, 265−275.
27. Echarte, M. M., Levi, V., Villamil, A. M., Rossi, R. C., and Rossi, J. P. F. C. (2001) *Anal. Biochem. 289*, 267−273.
28. Caride, A. J., Filoteo, A. G., Enyedi, Á., Verma, A. K., and Penniston, J. T. (1996) *Biochem. J. 316*, 353−359.
29. Graf, E., and Penniston, J. T. (1981) *J. Biol. Chem. 256*, 1587−1592.
30. Penniston, J. T. (1982) *Biochim. Biophys. Acta 688*, 735−739.
31. Kuzmic, P. (1996) *Anal. Biochem. 237*, 260−273.
32. Knott, G. (1996) *A Mathematical Modeling Laboratory; MLAB Applications Manual*, Civilized Software, Inc., Bethesda, MD.
33. Graf, E., Verma, A. K., Gorski, J. P., Lopaschuk, G., Niggli, V., Zurini, M., Carafoli, E., and Penniston, J. T. (1982) *Biochemistry 21*, 4511−4516.
34. Kosk-Kosicka, D., and Bzdega, T. (1990) *Biochemistry 29*, 3772−3777.
35. Vorherr, T., Kessler, T., Hofmann, F., and Carafoli, E. (1991) *J. Biol. Chem. 266*, 22−27.
36. Niggli, V., Penniston, J. T., and Carafoli, E. (1979) *J. Biol. Chem. 254*, 9955−9958.
37. Roth, S. M., Schneider, D. M., Strobel, L. A., VanBerkum, M. F. A., Means, A. R., and Wand, A. J. (1991) *Biochemistry 30*, 10078−10084.
38. Torok, K., Cowley, D. J., Brandmeier, B. D., Howell, S., Aitken, A., and Trentham, D. R. (1998) *Biochemistry 37*, 6188−6198.
39. Török, K., Tzortzopoulos, A., Grabarek, Z., Best, S. L., and Thorogate, R. (2001) *Biochemistry 40*, 14878−14890.
40. Sun, H., and Squier, T. C. (2000) *J. Biol. Chem. 275*, 1731−1738.
41. Kosk-Kosicka, D., and Bzdega, T. (1988) *J. Biol. Chem. 263*, 18184−18189.
42. Kosk-Kosicka, D., Bzdega, T., and Wawrzynow, A. (1989) *J. Biol. Chem. 264*, 19495−19499.
43. Levi, V., Rossi, J. P. F. C., Castello, P. R., and Flecha, F. L. G. (2000) *FEBS Lett. 483*, 99−103.
44. Gao, J., Yao, Y., and Squier, T. C. (2001) *Biophys. J. 80*, 1791−1801.
45. Ba-Thein, W., Caride, A. J., Enyedi, Á., Pászty, K., Croy, C. L., Filoteo, A. G., and Penniston, J. T. (2001) *Biochem. J. 356*, 241−245.
46. Brown, S. E., Martin, S. R., and Bayley, P. M. (1997) *J. Biol. Chem. 272*, 3389−3397.
47. Peersen, O. B., Madsen, T. S., and Falke, J. J. (1997) *Protein Sci. 6*, 794−807.
48. Paszty, K., Penheiter, A. R., Verma, A. K., Padanyi, R., Filoteo, A. G., Penniston, J. T., and Enyedi, A. (2002) *J. Biol. Chem. 277*, 36146−36151.

BI027098+